

## **EXPERIMENTAL STUDIES ON FLUID DYNAMICS BASED ON US M-LINE SIGNAL PROCESSING**

G. BAMBI, F. GUIDI, R. KRAMS\*, A. F.W. VAN DER STEEN\*  
and P. TORTOLI

University of Florence, Via Santa Marta 3, 50139 Firenze, Italy

\* Dept. Biomedical Engineering, Erasmus MC, 3000 DR Rotterdam

### **1. Introduction**

Multigate Doppler techniques can provide accurate information about blood velocity distribution along an M-mode line and could be used for diagnosis of atherosclerotic plaques. Since atherosclerosis is located in curvatures and near side-branches, we evaluated the accuracy of this technique in curved phantoms. As no analytical solution for the velocity field is available, accurate computational fluid dynamics (CFD) was used as a reference. Doppler profiles were measured with a multigate system, in curved cylindrical segments of varying curvature, resembling the human arterial coronary system. Velocity profiles obtained from Doppler measurements differed by less than 12% from CFD derived velocity profiles.

The multigate Doppler technique has also been applied *in vivo* for investigation of flow behavior in the aorta and in the common carotid artery (CCA), with the aim of clarifying the evolution of the velocity profile during the cardiac cycle. In both cases, significant effects of vessel curvature have been found and are discussed here.

### **2. Materials and methods**

#### *Ultrasound system*

Probes with different frequencies have been used in *in vitro* and *in vivo* experiments, respectively. *In vitro*, we used a piezoelectric 16 MHz transducer (manufactured at the Institute of Fundamental Research, PAN, Warsaw), producing a beam narrower than 1 mm (-6dB) over a range of about 15 mm.

For aortic blood flow (ABF) investigations, a special esophageal probe (EP) manufactured by Sometec (Paris, France) was used. The CCA hemodynamics in healthy volunteers was studied by means of a pencil 8 MHz transducer, focused at about 20 mm.

In all cases, the piezoelectric element was excited through electrical circuits included in the radio-frequency front-end together with receiver amplifiers. Phase-

quadrature demodulation, allowing forward and reverse flows to be distinguished, provided two base-band signal components to the acquisition system.

#### *Acquisition-processing system*

The multigate processing system consists of a PCI-bus plug-in card (to be housed in a PC), including three sections. The first section performs analog conditioning of input signals provided by the US system; the second carries out acquisition by means of two ADCs; the third performs data managing and processing in a high speed Digital Signal Processor (DSP) associated with SDRAM and PCI channel.

For each pulse transmitted at PRF rate, the system digitizes up to 128 complex samples with 14-bit resolution. Processing is performed by the TMS320C6202 (Texas Instruments Inc., TX), that computes in real-time the true spectra of the Doppler signals related to the subsequent range cells. The computed power spectral densities are sent to the host PC for real-time display (spectral profiles). During real-time operation, it is always possible to store in a file all raw data acquired over a time interval several seconds long, for possible post-processing.

All real time and post processing operations are under user control by means of a bundled software, named GASP (Global Acquisition and Signal Processing) which consists of an integrated shell for Windows™ family operating system. It includes applications for post processing carried out in LabVIEW™ (National Instruments, Austin, Texas) and a Visual C++ (Microsoft, Washington) coded console for real-time data acquisition and visualization.

#### *Flow simulator*

A closed-loop hydraulic circuit was used where the height difference between an upper and a lower reservoir controls flow velocity. The test fluid was a water suspension of Orgasol® backscattering particles, with mean diameter of 10  $\mu\text{m}$ .

The measurement section included a polyethylene tube, with 3 mm inner diameter and 4 mm outer diameter, fixed to a Plexiglas template in such a way to present five possible different measurement sites: one straight tube and four bends with the following curvature radii: A) 47 mm, B) 23 mm, C) 43 mm, D) 27 mm. The tube was immersed in water to facilitate the interrogation by the US probe. A special device allowed accurate positioning of the probe in the plane of symmetry of the curved tube.

#### *CFD derived velocity profiles*

A 3D-mesh, equivalent to the geometry of the hydraulic phantom, was generated in a well-validated CFD package (Septran, Septra, Delft, The Netherlands). The mesh consisted of approximately 2600 elements distributed over 80 cross sections that formed a tube with a diameter of 3 mm [1]. The tube described an arc of a circle with the same radii of curvature described above. The cross sectional resolution of the mesh was 0.15  $\text{mm}^2$  in the middle of the tube increasing to 0.075  $\text{mm}^2$  at the wall. As the number of cross section was constant, the axial resolution changed with curvature and varied between 1.3 mm to 2.34, for a curvature of 23 mm to 47 mm, respectively.

The following boundary conditions have been defined: parabolic, steady inflow of 0.5 and 1.0 ml/s at the entrance of the vessel, constant stress gradient at the outlet and no-slip conditions at the mesh wall. The fluid was modeled as a Newtonian fluid with a density of  $1050 \text{ kg/m}^3$  and a viscosity of 1 cP.

### 3. Experiments

#### *In vitro experiments*

Since the *in vitro* experiments have been done in steady flow condition, mean spectral profiles computed averaging a large number ( $>100$ ) of instantaneous profiles were used to extract the velocity profiles.

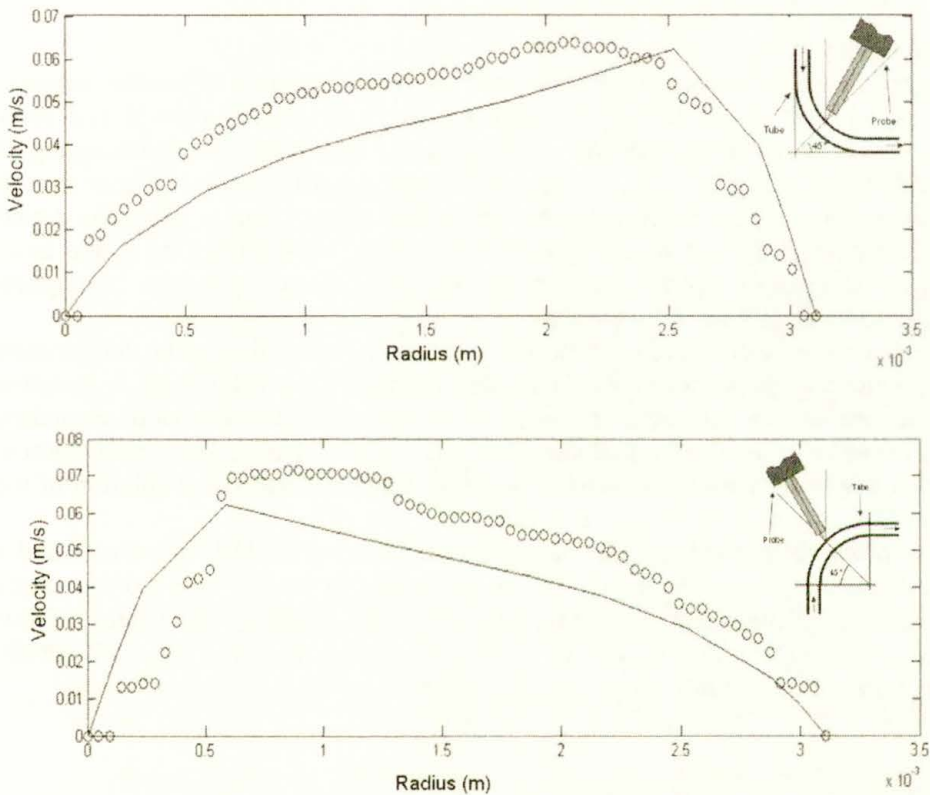


**Figure 1.** Comparison between Doppler (o) and CFD (-) derived velocity profiles for bends B (top) and D (bottom). Entrance conditions: 1 ml/s. Both results were evaluated in the middle cross section of the curved phantoms in order to minimize entrance/outlet effects. The relative positions of the transducer and the tube are shown in the upper right corner of each image.

For comparison of Doppler with CFD derived velocity profiles, we calculated the projection of the CFD derived 3D velocity vector on the direction of the US beam. The magnitude of the projected velocity vector ( $V_{\text{cfd}}$ ) was compared to the Doppler derived velocity ( $V_{\text{Doppler}}$ ) by calculating the normalized difference  $[(V_{\text{cfd}} - V_{\text{Doppler}})/V_{\text{Doppler}} * 100]$ . The difference between Doppler and CFD ( $\Delta_{\text{Doppler-cfd}}$ ) was defined as the average of this normalized difference (in %).

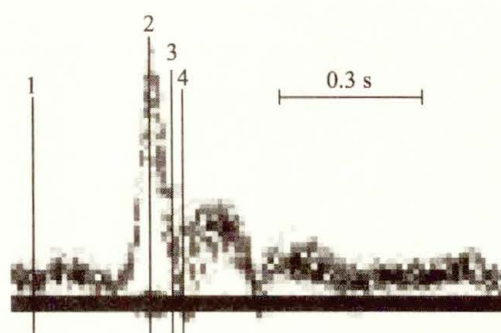
The Doppler derived velocity profiles behaved, in general, similar to the CFD derived velocity profiles with skewness (figure 1) increasing with entrance velocity and curvature. The differences between Doppler derived and CFD derived velocity profiles ( $\Delta_{\text{Doppler-cfd}}$ ) were small, ranging in the order of 5-12%, despite the large variations of haemodynamic conditions. The range of differences between CFD and Doppler derived velocity profiles was independent of entrance velocity and curvature.

### *In vivo experiments*

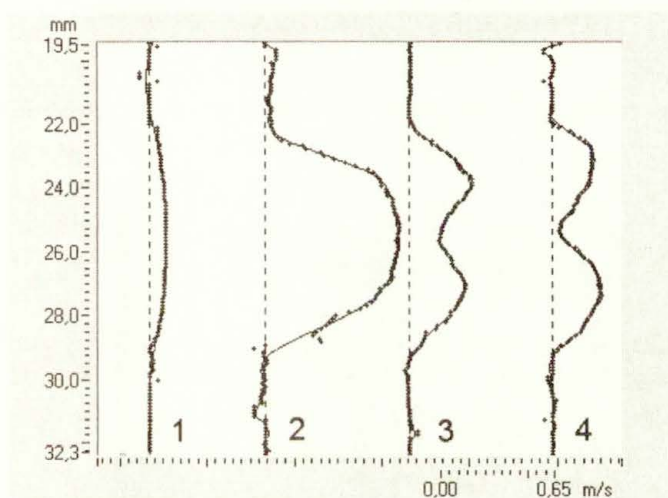
Experimental investigations in the common carotid arteries of healthy subjects have shown that blood velocity profiles are parabolic during diastole and early systole, and flat during the systolic peak. However, during late systole/beginning of diastole, they have an "M" shape, where the velocity near the walls is higher than in the vessel center (figure 2). Moreover, the profile shape changes when the sound beam direction is moved over a given cross-section, thus suggesting a non axis-symmetrical velocity distribution, which contradicts the straight tube assumption usually made for this artery.

This asymmetry of the velocity profile, especially evident during the deceleration phase following the systolic peak, has been noticed in 20 volunteers. A tentative explanation for such behaviour is given by correlating it to the growth of secondary flows caused by the slight vessel curvature and viscous effects. This explanation is supported by the comparison between *in vitro* results and numerical solution of the Navier-Stokes equations in laminar pulsed flow regime [2].

The probe for non-invasive hemodynamic monitoring of ABF in patients under general anesthesia or in the intensive care area, must be inserted at a thoracic depth where the esophagus and the aorta are nearby and parallel. The results of this investigation confirm that flow in the aorta is extremely complex, especially at the level of the aortic arch or in not-physiologic circumstances



(a)



(b)

**Figure 2.** (a) reference spectrogram of the Doppler signal produced by the maximum streamline velocity intercepted along the multigate scanline ; (b) velocity profiles corresponding to time instants highlighted in (a).

In general, the velocity profiles tend to be flat only during the systolic acceleration (figure 3), but not during the full cardiac cycle. In most cases they are asymmetrical, including both positive and negative components (figure 4). A marked skewness was always observed close to the arch. In particular, it has been shown [3] that appropriate positioning of the ultrasound transducer far from the arch curvature, is mandatory to make reliable ABF measurements. The real time display of the multigate system provides the means to inform the operator when such correct positioning is achieved.

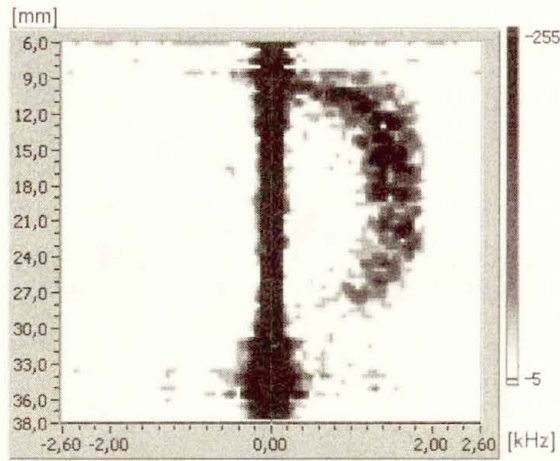


**Figure 3.** Typical instantaneous spectral profile detected during the systolic peak of the cardiac cycle.

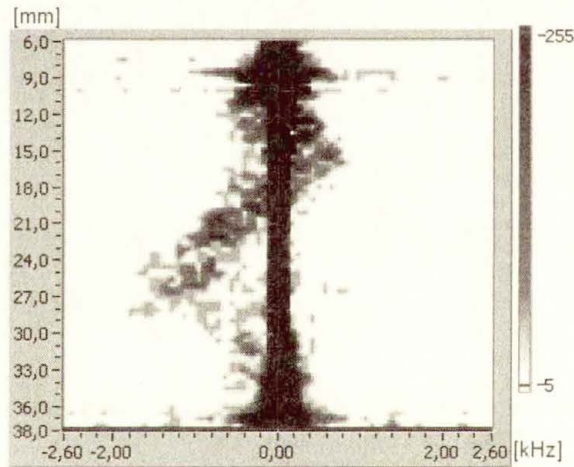


**Figure 4.** Instantaneous spectral profile obtained during systolic deceleration in a location close to the arch.

### Acknowledgement

This work was supported by the Italian Ministry of Education, University and Research (COFIN 2002).

### References

- [1] R. Krams, G. Bambi, F. Guidi, F. Helderma, A.F.W. van der Steen, P.Tortoli, Effect of vessel curvature on Doppler derived velocity profiles and fluid flow, submitted to *Ultrasound in Medicine and Biology*.
- [2] P.Tortoli, V. Michelassi, G. Bambi, F. Guidi, D. Righi, Interaction between secondary velocities, flow pulsation and vessel morphology in the common carotid artery, *Ultrasound in Medicine and Biology*, vol.29, n.3,pp.407-415, 2003.
- [3] P.Tortoli, G.Bambi, F. Guidi, R. Muchada, Towards a better quantitative measurement of aortic flow, *Ultrasound in Medicine and Biology*, vol.28, n.2, p.249-257, 2002.